General Disclaimer

One or more of the Following Statements may affect this Document

- This document has been reproduced from the best copy furnished by the organizational source. It is being released in the interest of making available as much information as possible.

- This document may contain data, which exceeds the sheet parameters. It was furnished in this condition by the organizational source and is the best copy available.

- This document may contain tone-on-tone or color graphs, charts and/or pictures, which have been reproduced in black and white.

- This document is paginated as submitted by the original source.

- Portions of this document are not fully legible due to the historical nature of some of the material. However, it is the best reproduction available from the original submission.

NASA Contractor Report 158985

APPLICATION OF HIGHER HARMONIC BLADE FEATHERING FOR HELICOPTER VIBRATION REDUCTION

Richard W. Powers

HUGHES HELICOPTERS
Division of Summa Corporation
Culver City, CA 90230

NASA Contract NAS1-14552
April 1978

National Aeronautics and Space Administration

Langley Research Center
Hampton, Virginia 23665

ABSTRACT

NASA/Langley Research Center has recently embarked on a comprehensive program of evaluating higher harmonic blade feathering for helicopter vibration reduction. Recent wind tunnel tests at the Langley Transonic Dynamics Wind Tunnel (TDT) have confirmed the effectiveness of higher harmonic control in reducing articulated rotor vibratory hub loads. Several predictive analyses developed in support of the NASA program have been shown to be capable of calculating single harmonic control inputs required to minimize a single 4P hub response. In addition, a multiple-input, multiple-output harmonic control predictive analysis has been developed in support of an upcoming wind tunnel investigation of this mode of higher harmonic control. All techniques developed thus far obtain a solution by extracting empirical transfer functions from sampled data. Algorithm data sampling and processing requirements are minimal to encourage adaptive control system application of such techniques in a flight environment. This paper is a status report on contract work to date.

TABLE OF CONTENTS

Introduction

The reduction of rotor-induced helicopter fuselage aeroelastic response carries with it the obvious benefits of enhanced operating life for critical aircraft components and reduced vibration of the controls and attendant pilot fatigue. Close examination of the rotor aerodynamic operating environment reveals the following: 1) rotor lift and drag and, hence, wake vorticity are a function of airstream velocity; 2) each rotor blade continually passes over its own wake and the wakes of other blades; 3) azimuthally varying vortex strengths and local airflows give rise to shear forces at the hub which are transmitted through the rotor shaft into the fuselage. Thus, blade root shears at harmonic multiples of the number of blades are the combined result of blade airloads, hub motion and various types of blade motion relative to the hub. As these shears transmit from the rotating to the non-rotating system of a 4-bladed helicopter, they give rise to the following:

1) 3P and 5P flapwise root shears result in 4P hub pitching and rolling moments.

2) 4P flapwise root shears feed into 4P shaft axial forces.

3) 3P and 5P chordwise root shears produce 4P hub fore-aft and lateral forces.

4) 4P chordwise root shears give rise to 4P hub yawing moments.

It can be shown for an n-bladed rotor system that, assuming all blades see the same loading at the same azimuth position, only $n\Omega$ frequency harmonics will be seen in the fixed system.

Thus, by utilizing phase relationships between various sources of rotor loads and introducing third, fourth and fifth harmonic pitch variations, the corresponding airload harmonics can be influenced. These airload harmonics, in turn, would influence blade motion and the modified motions and airloads together would modulate blade root shears. This is the premise upon which higher harmonic control is based, as illustrated in Figure 1.

For a four-bladed helicopter, higher harmonic pitch control as a means of vibration reduction requires superimposing 4P swashplate motion upon collective and cyclic control inputs. When external 4P control of the swashplate is present, third, fourth and fifth harmonic pitch variations may be obtained independently of the pilot's use of collective and first harmonic pitch. Fourth harmonic pitch can be achieved by oscillating the swashplate vertically as a fourth harmonic about the collective position set by the pilot. The technique

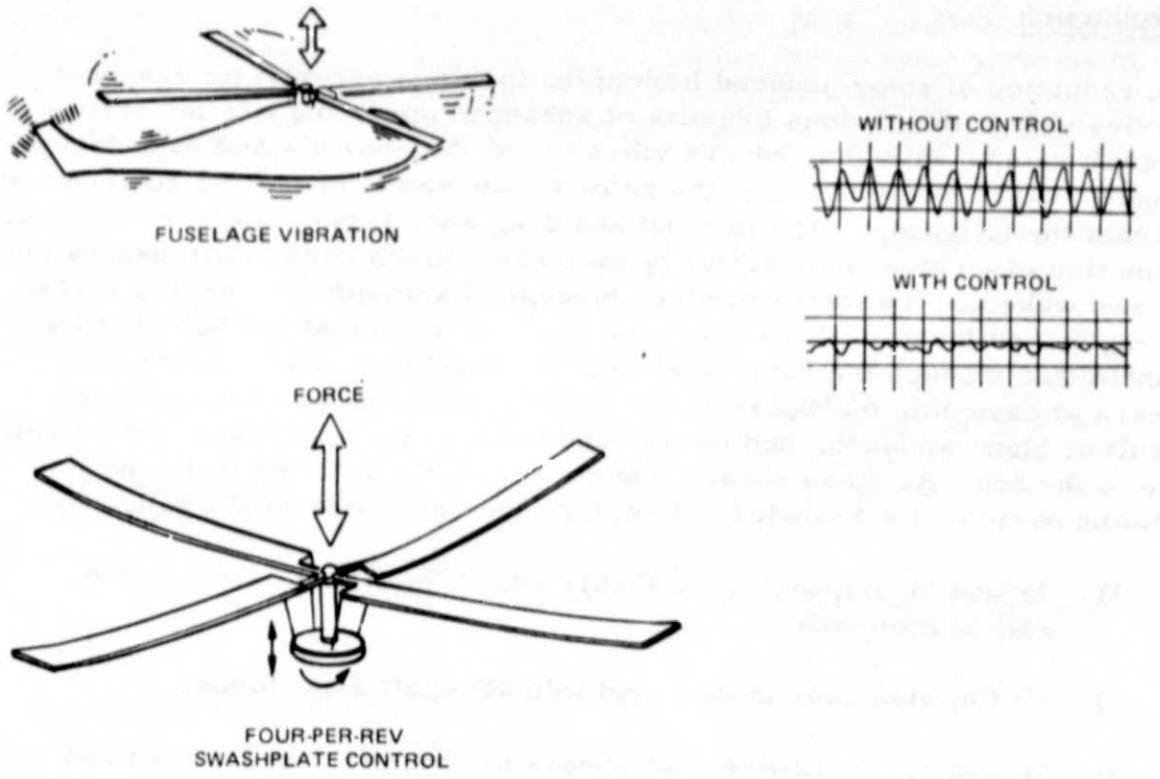

Figure 1. Helicopter Vibratory Loads Reduction by Higher Harmonic Control

for imposing third and fifth harmonic blade feathering involves fourth harmonic tilting of the swashplate. Consider the following blade pitch schedule $\theta(\psi)$ as a function of lateral swashplate tilt $\phi(\psi)$:

$$\theta(\psi) = \phi(\psi) \sin \psi \tag{1}$$

If swashplate tilt is allowed to vary as a fourth harmonic with amplitude A, then

$$\theta(\psi) = A \cos 4\psi \sin \psi$$

$$= \frac{A}{2} (\sin 5\psi - \sin 3\psi) . \tag{2}$$

If swashplate tilt is taken about a longitudinal axis, then,

$$\theta(\psi) = A \cos 4\psi \cos \psi$$

$$= \frac{A}{2} (\cos 5\psi + \cos 3\psi) . \qquad (3)$$

Similar results would be obtained if swashplate tilt was a sine phased fourth harmonic. It is clear, therefore, that any phase and magnitude combination of third and fifth harmonic pitch is possible by proper choice of amplitude and phase of fourth harmonic swashplate tilting about longitudinal and lateral axes.

The material that follows describes an investigation of several techniques developed under NASA contract NAS1-14552 to solve for required harmonic pitch amplitudes and phases. All algorithms developed thus far compute input signals required to null shaft oscillatory forces by extracting empirical transfer functions from sampled data. The various techniques are contrasted in terms of accuracy and their potential for application in a closed loop active control network.

Review of Previous Research

Emerging as the only flight test investigation of higher harmonic control for vibration reduction conducted to date, a 1962 test program described in Reference 1 employed an open-loop second harmonic blade feathering control system installed on a modified UH-1A. Provisions were made for in-flight adjustments of both amplitude and phasing of 2/rev blade feathering. Program objectives were threefold: 1) reduce vertical fuselage vibrations; 2) reduce oscillatory blade loads; and 3) delay the onset of retreating blade stall. Although the investigation of second harmonic control as a means of stall prevention was inconclusive, the program did demonstrate that a reduction in vertical vibration at the aircraft cg and a reduction in oscillatory blade bending moments can be achieved simultaneously through proper application of harmonic feathering.

A 1967 analytical investigation of higher harmonic pitch control to eliminate the transmission of oscillatory vertical forces from the rotor is detailed in Reference 2.

First the required pitch angles were found which eliminated oscillatory lift loadings at all radial stations by compensating for the azimuthal variation in blade tangential velocity and downwash nonuniformities. The assumed control system was such that radial and azimuthal variations in pitch angle inputs were possible.

Subsequent portions of the study were directed at computing pitch angle inputs at the blade root necessary to null oscillatory root shears. For this case, the constraint of eliminating oscillatory lift at all radial stations was relaxed.

Conclusions reached on the basis of analysis of a UH-1A-configured rotor were that radial schedules of higher harmonic pitch angles required to eliminate all oscillatory airloads were a function of flight condition, and would be difficult to accommodate such radial pitch variations in a flight application. The study also concluded that a majority of transmitted oscillatory vertical root shears can be eliminated by using only pitch angle inputs at second and fourth harmonics on a UH-1A.

An extension of the work performed in Reference 2 is described in Reference 3 in which oscillatory drag or inplane forces are addressed in addition to vertical vibratory loads. Elimination of oscillatory inplane loads was analytically achieved by superposing third and seventh blade feathering (second and sixth harmonic swashplate tilting motion) upon normal feathering requirements for trim. Reference 3 chose also to estimate the effect of higher harmonic pitch control inputs on performance. In concluding that the majority of vertical and inplane root shears can be eliminated simultaneously with second, third, fourth and seventh harmonic root pitch control, Reference 3 first demonstrated the feasibility of multiple-input, multiple-output higher harmonic control applications. In addition, results of Reference 3 support the contention that higher harmonic pitch control has little effect on rotor performance, a fact later to be borne out in wind tunnel investigations.

Although analytical treatments of higher harmonic control have established its feasibility, much of what is presently known about the technique has evolved through wind tunnel test programs. References 4, 5, 6, and 7 summarize wind tunnel investigations of harmonic control as well as the results generated from such programs.

References 4 and 5 describe a 1973 investigation, based on experimental frequency response data, of vibration compensation by periodic variations of the primary controls. Vibratory forces and moments to be compensated on the 2.29-m (7.5 ft) hingeless model were vertical force and pitching and rolling moments. Using transfer function methods in the frequency domain to calculate required control inputs as well as the resultant blade response, it was

found blade pitch variations required for vibration alleviation vary as a function of advance ratio; less than 1 degree for $0.2 \leq \mu \leq 0.45$ and 3 degrees for $\mu = 0.85$. The 4P compensation control inputs were effective in attenuating 3P and 5P flapwise bending moments while 2P flap moments were largely unaffected by 4P blade feathering. It is noted that References 4 and 5 report there was no instrumentation to measure vibratory hub pitching and rolling moments, and that these quantities were obtained from flapwise bending moments. Thus, the effect of inplane forces, vertical shear forces and blade torsion have been ignored. In addition, the effect of blade feathering on rotor performance was not addressed.

Reference 6 and its extension Reference 7 describes what has proven to be the most comprehensive and encouraging wind tunnel investigation of harmonic control to date. By imposing 4P swashplate vertical motion as well as pitching and rolling motion on a 3.05-m (10.0 ft) Mach-scaled hingeless rotor, it was observed that vibratory hub load reduction carries with it no penalty in terms of blade flap bending or rotor performance. While Reference 6 describes performance benefits of 20 percent with 2P feathering, Reference 7 reported no such improvement with 4P feathering.

Paramount in the conclusions of Reference 7 is the fact that simultaneous reduction of several vibratory hub load components is possible due to superposition of harmonic pitch effects, thus underscoring conclusions of Reference 3.

Although not discussed in previous work, high frequency blade pitching carries with it increased control loads by virtue of the tennis racket effect. In contrast, Multicyclic Flap Control, Reference 8, wherein high frequency elastic torsional deformations generated by a mid-span servo flap are employed to null hub vibratory loads, has no such penalty. Inertia-induced control loads, in fact, are greatly reduced since only a flap is being driven, not the blade. In addition, Reference 9 reports mid-span pitching is far more efficient than full span pitch control in reducing first mode flap bending excitation. Inherent design drawbacks of servo-flap control are greater mechanical complexity in terms of rotor blade/control system design integration.

Although the above studies as well as others not mentioned here, were successful in demonstrating the potential of harmonic control to expand the

flight envelope of the hingeless rotor there exists a need for further study in several areas. Specifically, this paper intends to address the following:

- The effect of 4P swashplate vertical, pitch and roll motion on hub forces and moments of an articulated rotor model in the wind tunnel.
- General characteristics of several algorithms developed to predict required swashplate inputs.
- Considerations for applying harmonic control in an active feedback network.

Wind Tunnel Testing

The solution techniques explored thus far have been developed in support of Langley Research Center's comprehensive program of evaluating active higher harmonic control for reduction of helicopter aeroelastic response. The program embodies the phases shown in Figure 2. The higher harmonic control concept was evaluated recently using a 2.74-m (9.0 ft) diameter aeroelastically scaled rotor model in the NASA/Langley Transonic Dynamics Wind Tunnel (TDT). Characteristics of the model rotor are given in Figure 3, Table I and Figure 4. The test was conducted such that manual phase and amplitude sweeps of 4P collective, longitudinal cyclic, and lateral cyclic feathering were made to explore the frequency response of the

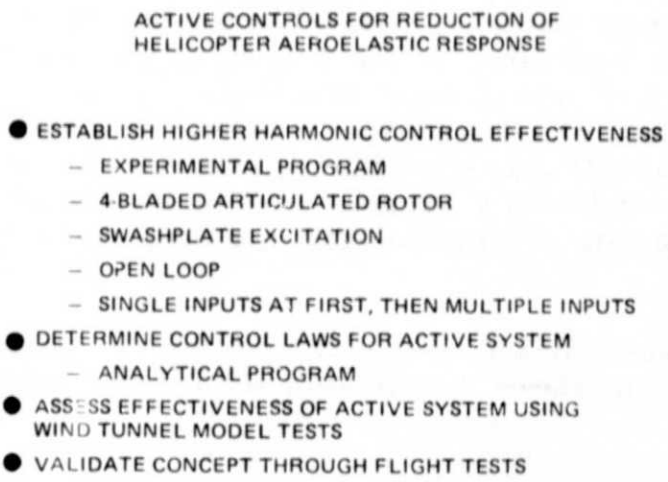

Figure 2. NLRC Active Higher Harmonic Control Program

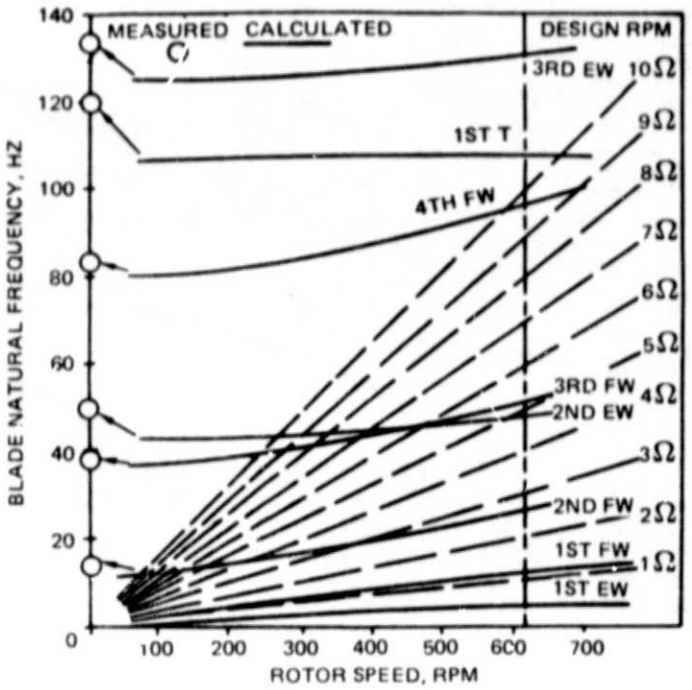

Figure 3. Blade Rotating Natural Frequency Characteristics

TABLE I. SUMMARY OF ROTOR SYSTEM PROPERTIES FOR THE 2.7-METER (9 FOOT) DIAMETER RESEARCH MODEL ROTOR SYSTEM

Rotor Type	Fully Articulated
Number of Blades	4
Rotor Diameter	279-cm (110 in.)
Blade Chord	10.77-cm (4.24 in.)
Spar Chord	4.72-cm (1.86 in.)
Solidity	0.0982
Airfoil Section	NACA 0012
Theoretical Blade Twist	0 degrees
Hinge Offset, Coincident	7.62-cm (3.0 in.)
Root Cutout	31.75-cm (12.5 in.)
Blade Elastic Axis	25% Chord Nominal
Blade Pitch Axis	25% Chord
Center of Gravity	Adjustable (Outer Blade 22% thru 37%)

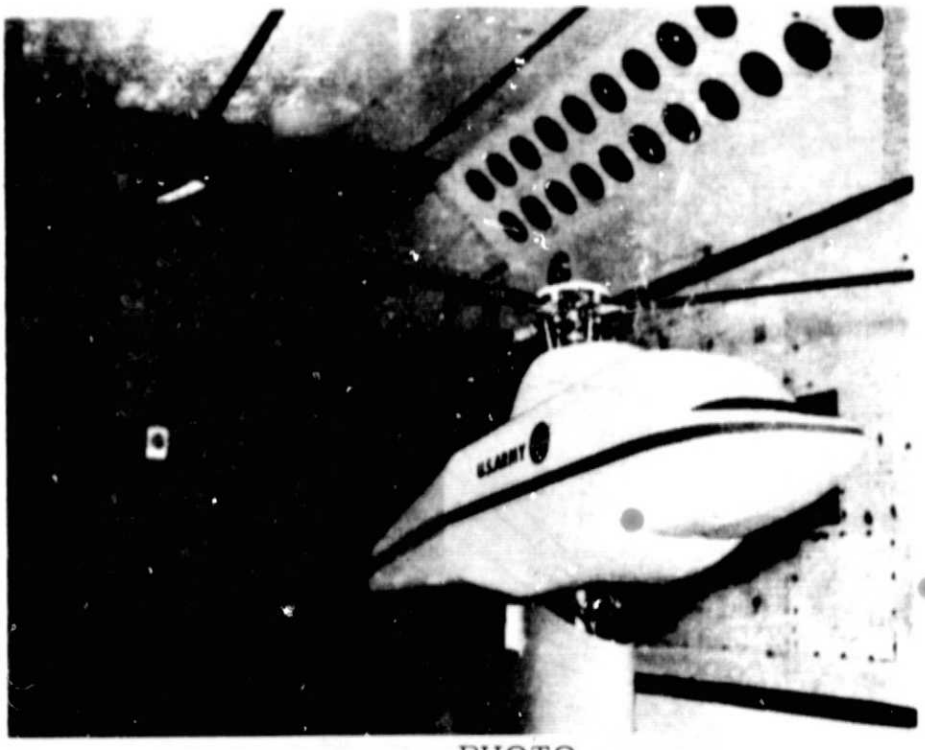

PHOTO

Figure 4. Aeroelastic Experimental Rotor System

six hub forces and moments. Combined rotor/fuselage responses were measured by a six-component balance mounted below the pylon. Hub vibratory loads as measured by the balance were corrected to compensate for non-scale swashplate inertial forces. Blade and pitch link loads were also monitored.

Figures 5 and 6 depict a representative variation of 4P hub normal response with 4P collective feathering inputs. Azimuthal and radial coordinates of the Figure 4 phasor plot represent 4P hub normal response phase and magnitude, respectively. Sample 4P collective inputs were made at a constant amplitude of 1/2 degree, the data points being annotated with input phase. Baseline hub response represents the ambient hub response to be compensated prior to any feathering inputs. Figure 6 illustrates an optimization technique by which a local minimum can be reached by varying 4P input phase, and further refined by modulating 4P input amplitude.

Preliminary wind tunnel results concerning the effect of 4P feathering inputs on blade loads are presented in Figures 7 through 12, and discussed

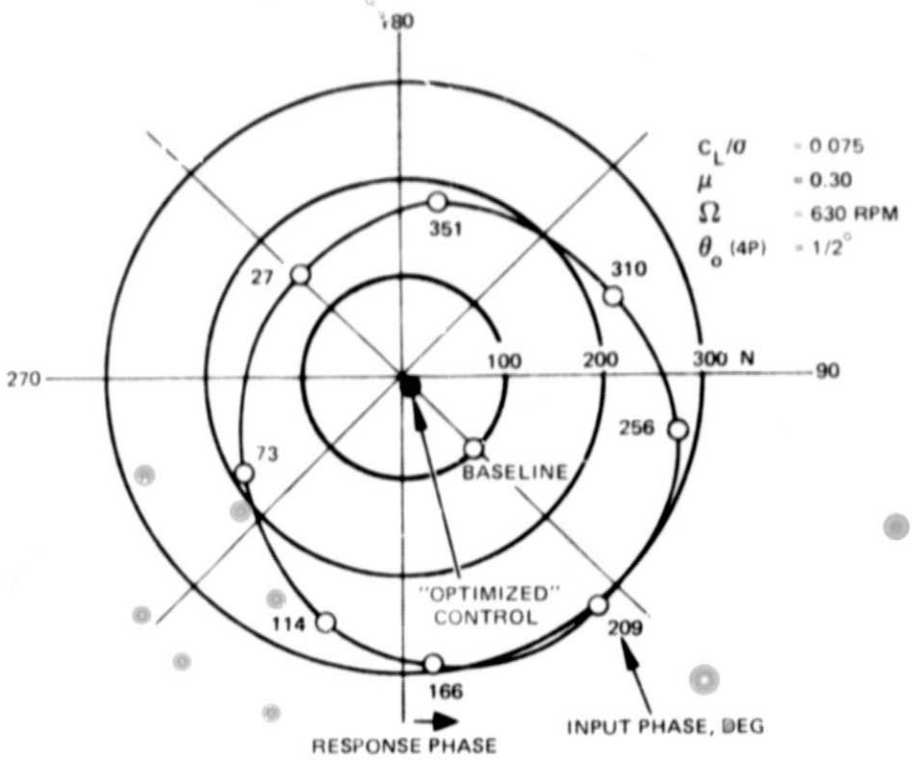

Figure 5. Variation of 4/Rev Normal Force with 4/Rev Collective Input Phase

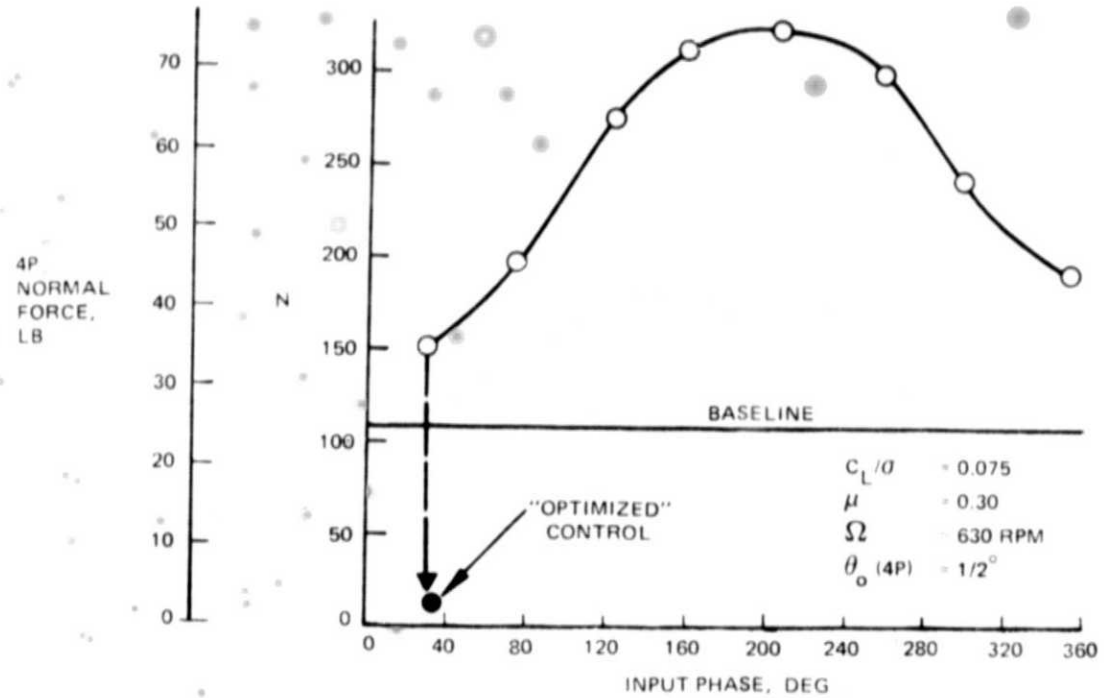

Figure 6. Variation of 4/Rev Normal Force with 4/Rev Collective Input Phase

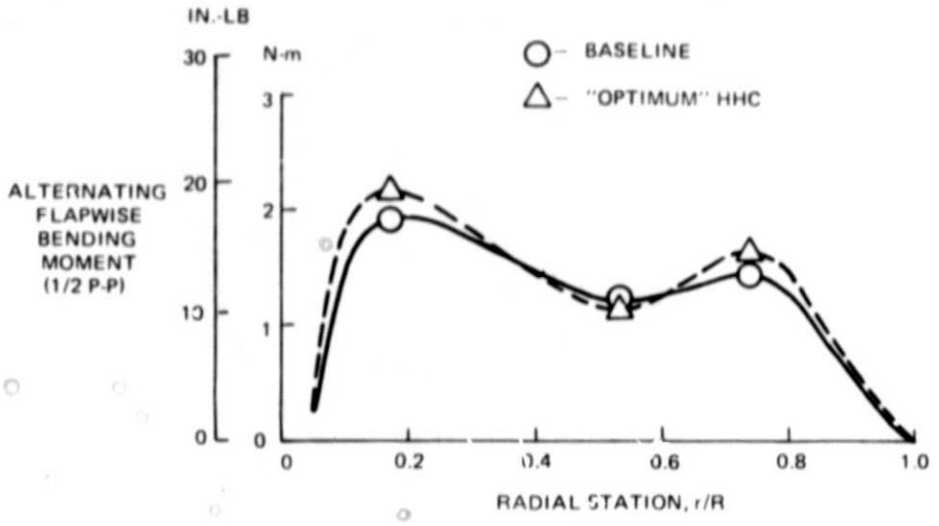

Figure 7. Spanwise Variation of Blade Alternating Flapwise Moment (Ref. 10)

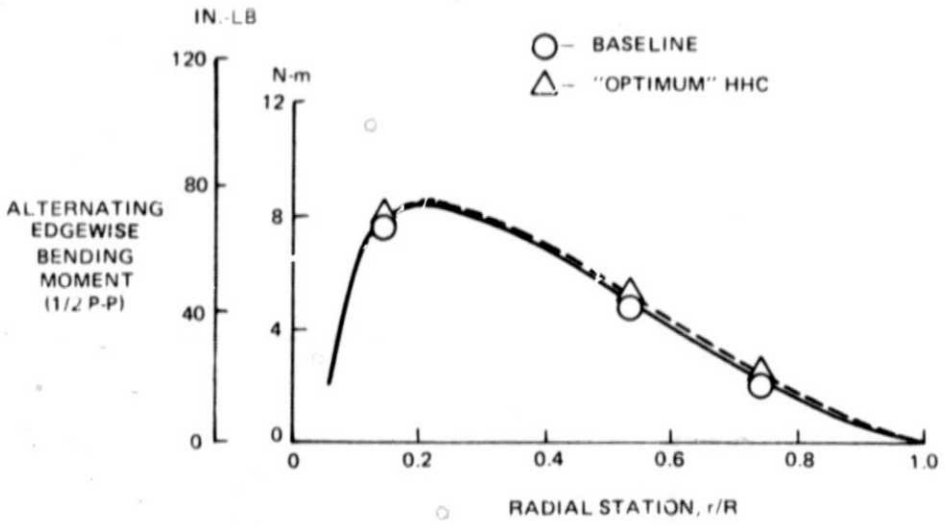

Figure 8. Spanwise Variation of Blade Alternating Edgewise Moment (Ref. 10)

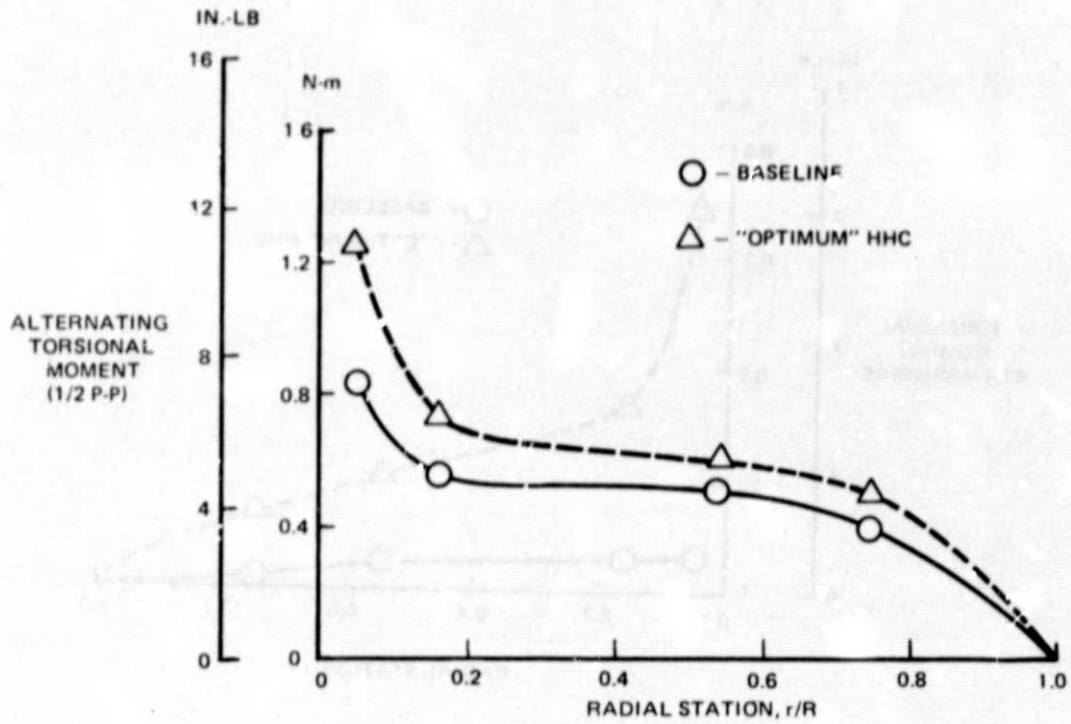

Figure 9. Spanwise Variation of Blade Alternating Torsional Moment (Ref. 10)

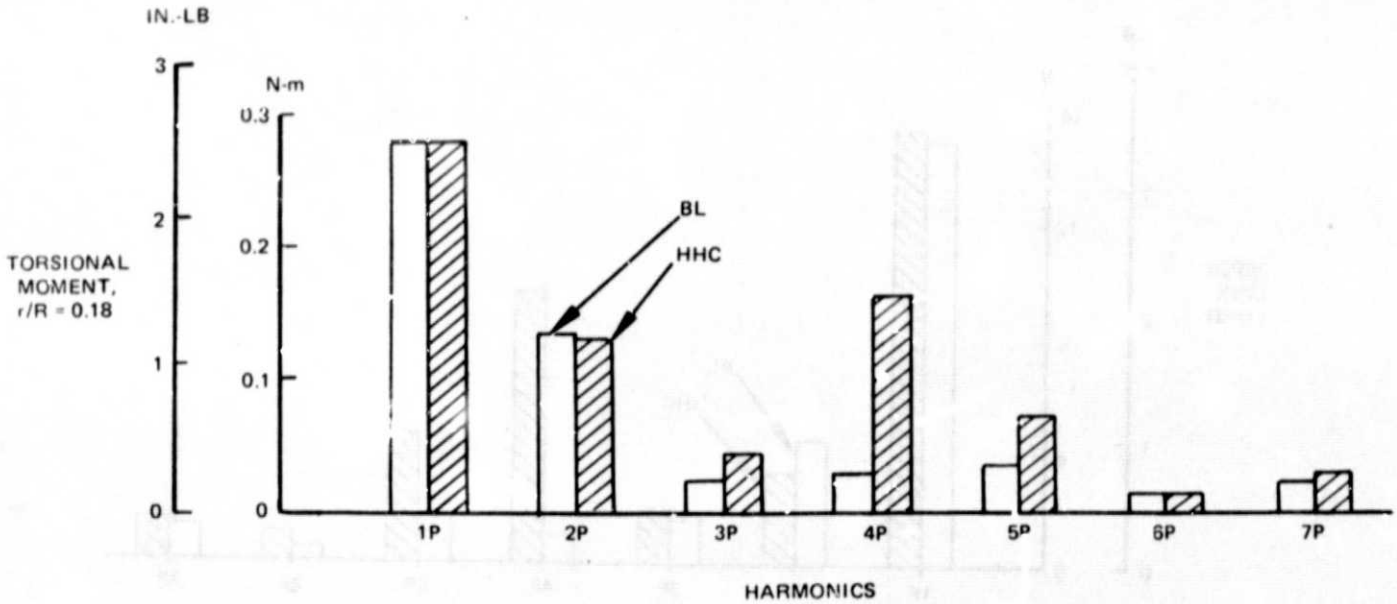

Figure 10. Harmonic Decomposition of Blade Torsional Moment (Ref. 10)

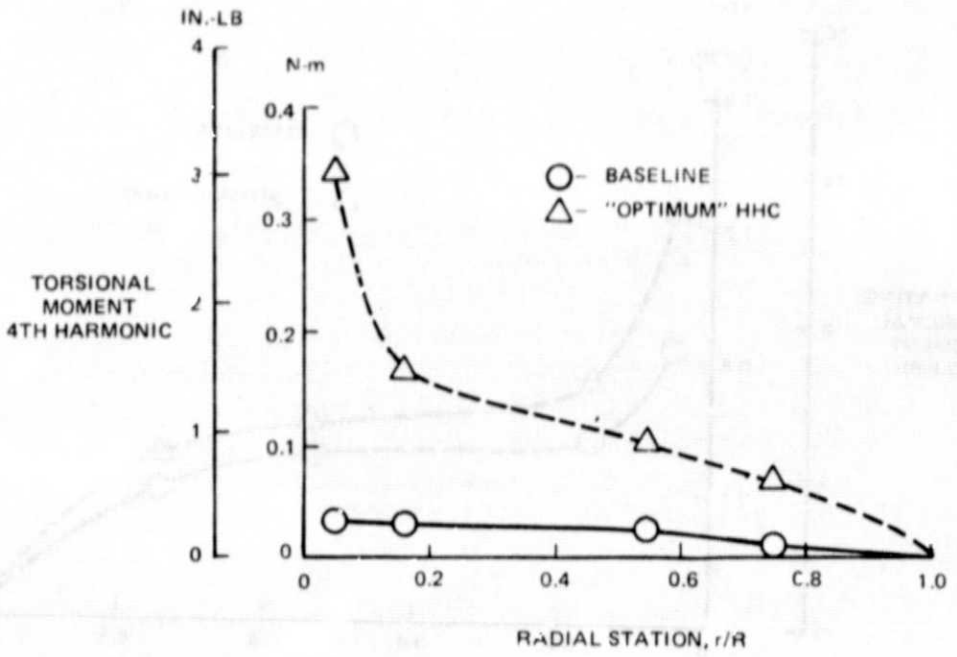

Figure 11. Spanwise Variation of Blade Torsional Moment Fourth Harmonic (Ref. 10)

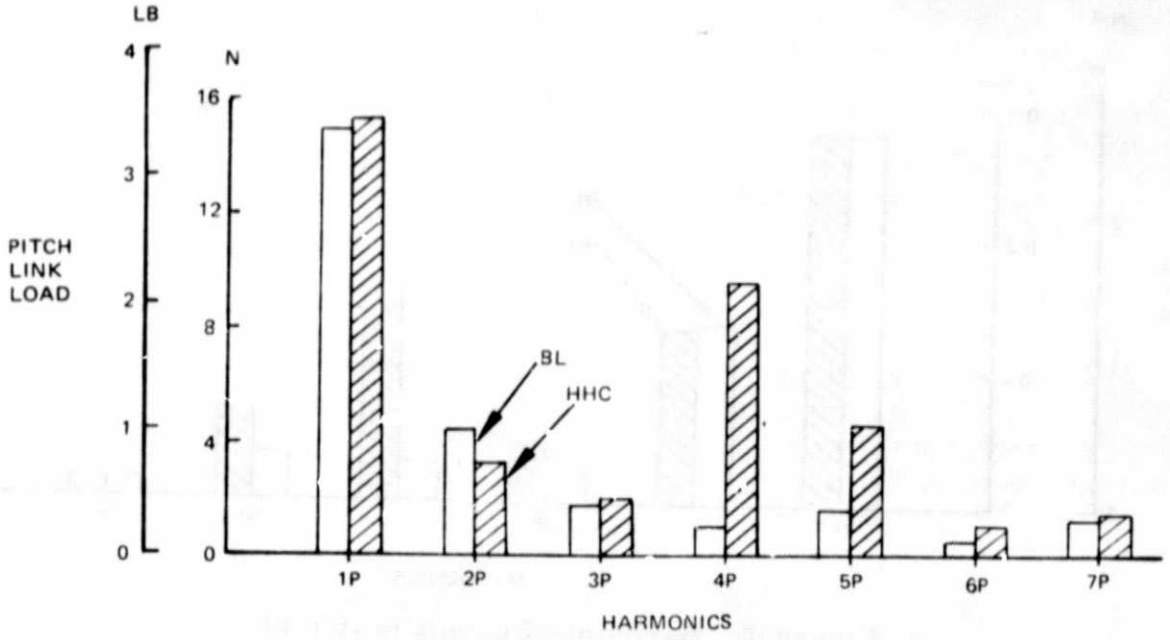

Figure 12. Harmonic Decomposition of Pitch Link Load (Ref. 10)

in greater detail in Reference 10. It was found that although flapwise and edgewise bending moments were fairly insensitive to 4P collective inputs at the "optimized" condition of Figure 6 (0.22 degree amplitude, 30 degree phase), root torsional moments and, hence, pitch link loads were aggravated by such inputs, as illustrated in Figure 9. Specifically, the 4P content of blade torsional moment and pitch link load was highly amplified as a result of feathering induced inertial loads, Figures 10, 11, and 12.

As noted in Figure 3, however, the first elastic torsion mode of the blade was above 10P at the design operating speed. Thus, a more torsionally compliant rotor may not have undergone such dynamic amplifications in pitch link loading. The substantial increase in 5P content of torsional moment and pitch link load, as depicted in Figures 10 and 12, can be attributed to inadvertent mixing of 4P collective signals with swashplate pitching and rolling motion.

By way of conclusion, wind tunnel testing of a dynamically scaled model rotor has established that higher harmonic blade feathering can minimize rotor-transmitted hub vibratory forces and moments. Although such feathering inputs may result in higher blade and control system loads, judicious blade design may provide relief from any loading penalties.

Predictive Analysis Overview

The effectiveness of higher harmonic control having been established through wind tunnel testing described in the previous section, a deterministic approach to solving for required feathering inputs is developed next. The desire to implement higher harmonic control in an adaptive control system has created a set of unique requirements for solution techniques. Algorithms to be employed must be efficient so as to permit a high solution refresh rate. In addition, the algorithm must require a minimum of sampled data, both in quantity and type, so as not to impose burdensome data acquisition requirements. Working within these requirements, there exist several control philosophies that can be accommodated:

- A single swashplate degree of freedom (d.o.f.) is used to control a single hub response.
- A single swashplate d.o.f. is used to control an aggregate of hub responses.

- Multiple swashplate d. o. f. 's are used to control a single hub response.
- Multiple swashplate d. o. f. 's are used to control multiple hub responses.

In addition, any one of these techniques may be implemented using multiple frequencies (i. e., 4P, 8P, and 12P blade pitching).

Several predictive techniques have been developed to treat the single input, single output higher harmonic control philosophy. These techniques were developed in support of the 1977 NLRC TDT test program, and, consequently, results have been generated from available data. Techniques dealing with multiple-input, multiple-output harmonic control have similarly been developed for a planned March 1978 TDT test program. The various techniques will be developed and contrasted in the sections that follow.

Single Input, Single Output Predictive Analyses

Three-Point Technique

In developing predictive algorithms to calculate optimal swashplate inputs, advantage was taken of the almost linear relationship between 4P feathering inputs and 4P hub oscillatory forces and moments. The first such approach developed requires a priori knowledge of baseline vibration levels and two samples of oscillatory output in response to known 4P feathering inputs. By using 4P collective swashplate inputs to minimize 4P hub normal forces, the procedure can be outlined as follows:

1) Define feathering inputs and response quantities as phasors having magnitude and phase as:

$$\bar{F}_{ZBL} = (|\bar{F}_{ZBL}| \cdot \phi_{ZBL})$$

Phasor representing 4P component of baseline hub normal force, with amplitude $|\bar{F}_{ZBL}|$ and phase relative to an index blade ϕ_{ZBL}

$\bar{F}_{Z1} = (|\bar{F}_{Z1}|, \phi_{Z1})$ — Phasor representing 4P component of hub normal force in response to an arbitrary 4P collective input

$\bar{F}_{Z2} = (|\bar{F}_{Z2}|, \phi_{Z2})$ — Phasor representing 4P component of hub normal force in response to an arbitrary 4P collective input different from above

$\bar{\theta}_{01} = (|\bar{\theta}_{01}|, \Delta\phi_{01})$ — Phasor representing the first arbitrary 4P collective perturbation with magnitude $|\bar{\theta}_{01}|$ and phase $\Delta\phi_{01}$

$\bar{\theta}_{02} = (|\bar{\theta}_{02}|, \Delta\phi_{02})$ — Phasor representing a second arbitrary 4P collective perturbation

2) Transform phase and amplitude to sine and cosine magnitudes:

$$F_{ZCBL} = |\bar{F}_{ZBL}| \cos \phi_{ZBL}$$

$$F_{ZSBL} = |\bar{F}_{ZBL}| \sin \phi_{ZBL}$$

$$\theta_{OC_1} = |\bar{\theta}_{01}| \cos \Delta\phi_{01}$$

$$\theta_{OS1} = |\bar{\theta}_{01}| \sin \Delta\phi_{01}$$

$$\vdots$$

etc.

3) Assume there exists a plane, Figure 13, that describes the relationship between 4P hub normal force cosine magnitude and 4P swashplate collective sine and cosine magnitudes. Assume a similar plane exists for the sine magnitude of 4P hub normal force. In addition, establish the following limitations:

   a) The F_{ZC} and F_{ZS} planes are not parallel to each other

   b) Neither of the two planes are parallel to the plane of zero response ($F_{ZC} = F_{ZS} = 0$)

   c) The locus of points representing the intersection of the planes is not parallel to the plane of zero response.

4) Write equations for the F_{ZC} and F_{ZS} planes in terms of two arbitrary coefficients and baseline magnitudes.

$$A\theta_{OC} + B\theta_{OS} + (F_{ZC} - F_{ZCBL}) = 0 \quad (4)$$

$$D\theta_{OC} + E\theta_{OS} + F_{ZS} - F_{ZSBL}) = 0 \quad (5)$$

   By substituting two frequency response samples, the coefficients in Equation (4) and Equation (5) may be determined.

5) Referring to Figure 13, F_{ZC} and F_{ZS} in Equations (4) and (5), respectively, may now be set to zero. This yields equations for two lines in the zero-response plane, represented by line segments $\overline{AB}$ and $\overline{CD}$ in Figure 13. Simultaneous solution of the two equations yields point P, whose coordinates are the sine and cosine magnitudes of the 4P collective input needed to null the sine and cosine magnitudes of hub response.

A schedule of 4P collective inputs and resulting 4P hub normal force responses for a particular wind tunnel trim condition is presented in Table II. Test conduct was such that 4P collective amplitude was held constant while phase was swept manually in near 45 degree increments. Table III presents results using data from Table II with the 3-point technique. Results were calculated based on combinatorial permutations of two of the eight available data points to check solution consistency. A single

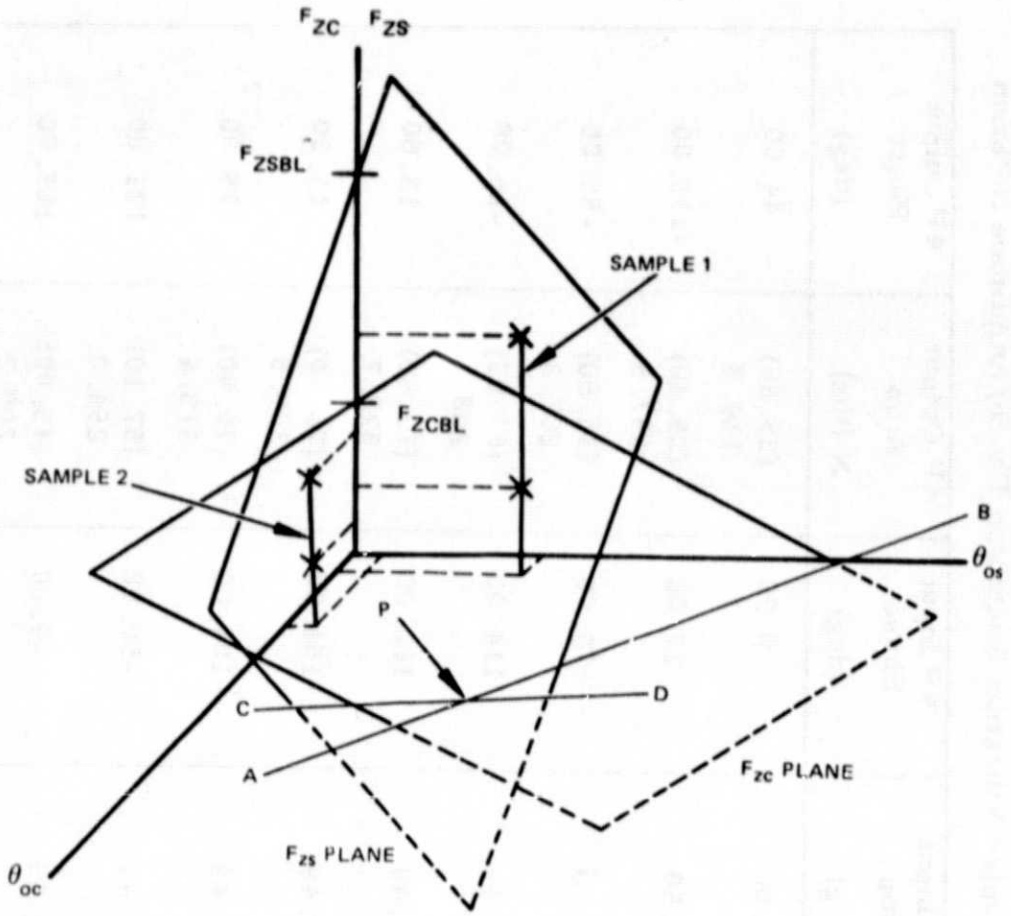

Figure 13. Planar Relationships Between 4P Collective Input and 4P Shaft Axial Force Sin and Cos Components

solution was then obtained by neglecting those solutions with phase greater than one standard deviation away from the mean phase. A new mean phase and amplitude was then calculated from the reduced set of solutions. Results generated from test data were fairly consistent with three exceptions noted. Close examination revealed that when 4P perturbations were made 180 degrees apart, as were the 3 cases of Table III, the planes that resulted were vertical and coplanar, thereby defining an infinite set of non-unique solutions. Rather than impose a sampling scheme to preclude 180 degree-apart sampling, it was deemed more appropriate to develop a technique that has no such constraints.

TABLE II. SCHEDULE OF 4P COLLECTIVE INPUTS AND HUB RESPONSES

$\mu = 0.30 \quad C_L/\sigma = 0.075$

Higher Harmonic Blade Feathering for Helicopter Vibration Reduction Phase/Amplitude Notation

Point	Response of Interest	4P Input Amp (deg)	4P Input Phase (deg)	4P Output Amp N (lbs)	4P Output Phase (deg)
213	Baseline/Normal Force	0.00	0.00	(25.80) 114.8	44.00
214	Collective/Normal Force	0.50	27.00	(35.40) 157.5	-138.00
215	Collective/Normal Force	0.50	73.00	(46.60) 207.3	-59.00
216	Collective/Normal Force	0.49	114.00	(65.00) 288.1	-26.00
217	Collective/Normal Force	0.49	166.00	(73.90) 328.7	13.00
218	Collective/Normal Force	0.49	-151.00	(76.40) 339.8	41.00
219	Collective/Normal Force	0.48	-104.00	(70.90) 315.4	75.00
220	Collective/Normal Force	0.49	-50.00	(57.10) 254.0	121.00
221	Collective/Normal Force	0.49	-9.00	(45.00) 200.2	165.00

TABLE III. SOLUTION INPUTS BASED ON 3-POINT TECHNIQUE
(DATA FROM TABLE II)

Three-Point Higher Harmonic Solution

Data from Cases		4P Input Amplitude	4P Input Phase
214	215	0.211	28.100
214	216	0.210	28.132
214	217	0.210	28.224
214	218	0.197	26.131
214	219	0.211	28.374
214	220	0.210	28.220
214	221	0.210	28.084
215	216	0.251	26.286
215	217	0.251	25.268
215	218	0.251	32.355
215	219 ←	0.361	91.018
215	220	0.241	23.078
215	221	0.223	28.452
216	217	0.250	24.543
216	218	0.251	32.710
216	219	0.241	40.101
216	220 ←	0.218	13.641
216	221	0.208	29.913
217	218	0.251	33.437
217	219	0.244	31.596
217	220	0.264	28.002
217	221 ←	0.102	87.186
218	219	0.250	33.180
218	220	0.252	33.091
218	221	0.256	32.975
219	220	0.231	34.196
219	221	0.220	34.396
220	221	0.208	34.652

Linear Higher Harmonic Solution

4P Input Amplitude	4P Input Phase
0.232	30.140

Nonlinear (Six-Point) Technique

The second predictive approach to be investigated replaces the planes of the former approach with second-order surfaces defined by equations 6 and 7:

$$A\theta_{OC}^{2} + B\theta_{OS}^{2} + C\theta_{OC}\theta_{OS} + D\theta_{OC} + E\theta_{OS} = F_{ZC} - F_{ZCBL} \qquad (6)$$

$$F\theta_{OC}^{2} + G\theta_{OS}^{2} + H\theta_{OC}\theta_{OS} + I\theta_{OC} + J\theta_{OS} = F_{ZS} - F_{ZSBL} \qquad (7)$$

The shape functions above are similar to cubic polynomials used in finite element plate analysis; the lower-order terms are retained to improve the approximation while higher-order terms are eliminated to reduce the number of samples required to define coefficients A through J.

In addition to a baseline condition, five sample swashplate inputs and resulting hub responses are required to uniquely define the two shape functions. Once the 10 coefficients are defined, a Newton-Raphson iterative scheme is used to solve the set of nonlinear algebraic equations for the required swashplate inputs. The scheme takes the following recursive form:

$$\{\theta\}_{i+1} = \{\theta\}_{i} - [\nabla f]_{i}^{-1} \{f\}_{i} \qquad i = 1, \ldots, N \qquad (8)$$

where

$$\{\theta\}_{i} = \begin{Bmatrix} \theta_{OC} \\ \theta_{OS} \end{Bmatrix}_{i}$$

$$[\nabla f]_{i} = \begin{bmatrix} 2A\theta_{OC} + 2\theta_{OS} + D & 2B\theta_{OS} + C\theta_{OC} + E \\ 2F\theta_{OC} + H\theta_{OS} + I & 2G\theta_{OS} + H\theta_{OC} + J \end{bmatrix}_{i}$$

and N is the number of iterations. The analysis is initiated (i = o) by using solution inputs derived from the linear 3-point technique or a reasonable guess. A satisfactory tolerance on convergence can usually be met in 4-5 iterations. Table IV presents results generated from Table II data using the nonlinear approach. Good agreement is seen between the linear and nonlinear algorithms, indicating hub forces are more linear than nonlinear with control inputs of small amplitude.

The need for five data points as well as a baseline does not preclude active control applications of a nonlinear approach. Reference 11 details a minicomputer-directed helicopter active control network where up to 24 samples of rotor state were required each revolution. In the event a particular control application was unable to sustain the rather low 6 samples/rev rate, the process could be retarded to provide a new solution every several revolutions. The lowered solution rate would virtually be undetectable in the cabin environment.

The paramount drawback to this type of analysis lies in its arduous data processing requirements. The inversion of 5 by 5 matrices coupled with an iterative solution process could erode control loop response. Thus, a third predictive analysis was investigated which has no inherent sampling constraints nor exhaustive data processing requirements.

Two-Point Technique

The third single-input, single output algorithm to be investigated requires a baseline and only one sample frequency response to provide a solution. The technique, developed by Langley, is based on the following tacit assumption: if higher harmonic partial response is defined as that portion of hub

TABLE IV. SOLUTION INPUT BASED ON 6-POINT NONLINEAR TECHNIQUE (DATA FROM TABLE II)

Nonlinear Higher Harmonic Solution
Using Newton-Raphson Iteration

Number of Iterations = 3

Data from Cases	4P Input Amplitude	4P Input Phase
214, 215, 216, 217, 218	0.223	29.514

•scillatory force due solely to 4P feathering inputs (i.e., total response minus baseline response), then 4P sample input phase leads harmonic partial response phase by a constant amount. The validity of this assumption using Table II data is established in Table V. Referring to Figure 14, the algorithm can be summarized as follows:

1) Using phasor notation, vectorially subtract the baseline hub response of interest from the perturbation hub response.

$$\bar{F}_{ZHH} = \bar{F}_{Z1} - \bar{F}_{ZBL} \tag{9}$$

TABLE V. ASSUMPTION: SAMPLE INPUT PHASE LEADS HIGHER HARMONIC CONTROL PARTIAL RESPONSE PHASE BY CONSTANT AMOUNT

4P Collective Input Phase, deg	4P HHC Partial Response Phase	Δ
27	222	196
73	275	202
114	310	197
166	358	193
209	32	190
256	90	194
310	147	197
351	185	194

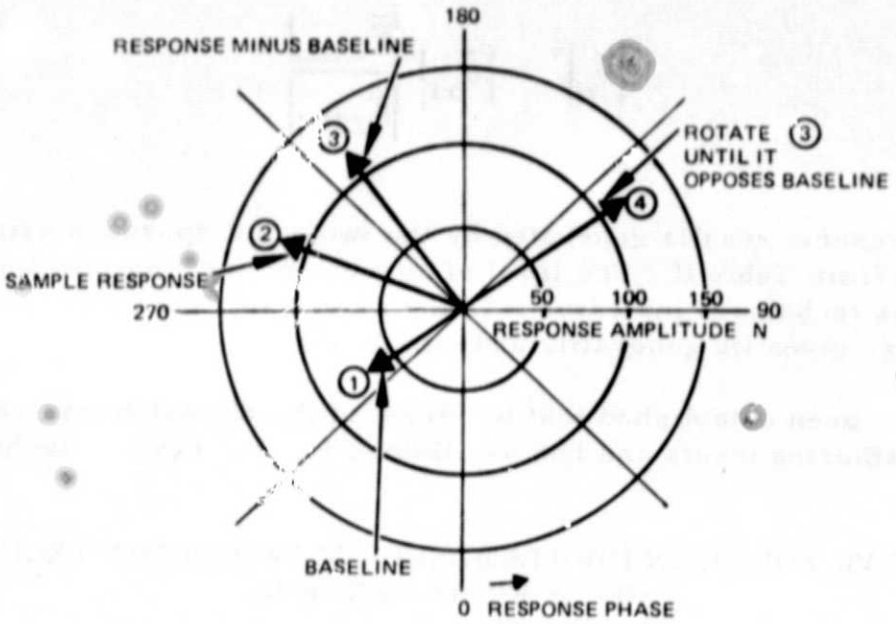

Figure 14. Two-Point Higher Harmonic Solution Technique

2) Rotate the higher harmonic partial response phasor until it opposes the baseline phasor. If $\bar{F}_{ZHH}$ has magnitude and phase $|F_{ZHH}|$ and θ_{ZHH}, this step requires a rotation of magnitude $\theta_{ZHH} - (\phi_{ZBL} - 180)$.

3) By virtue of the assumption that the difference between control input phase and harmonic control partial response phase is constant for a given flight condition, the required control input phase may be written

$$\Delta\phi_o^* = \Delta\phi_{od} - (\theta_{ZHH} - (\phi_{ZBL} - 180)) \qquad (10)$$

4) Allowing that harmonic control partial response magnitude $|\bar{F}_{ZHH}|$ is linear with control input amplitude, the required control input amplitude for nulling baseline response is

$$\left|\bar{\theta}_o\right|^* = \left|\bar{\theta}_{o1}\right| \frac{\left|\bar{F}_{ZBL}\right|}{\left|\bar{F}_{ZHH}\right|} \tag{11}$$

Table VI presents results generated by the two-point approach using wind tunnel data from Table II. The level of agreement between this approach and the previous techniques indicates it is the most likely candidate for control applications, given its generality and simplicity.

Thus, it has been established that by virtue of the almost linear relationship between feathering inputs and hub oscillatory forces, several techniques

TABLE VI. SOLUTION INPUTS BASED ON TWO-POINT TECHNIQUE (DATA FROM TABLE II)

Two-Point Higher Harmonic Solution

Data from Case	4P Input Amplitude	4P Input Phase
214	0.210	28.156
215	0.221	21.627
216	0.206	27.343
217	0.236	31.391
218	0.249	33.527
219	0.244	29.763
220	0.221	26.891
221	0.202	29.222

Linear Higher Harmonic Solution

4P Input Amplitude	4P Input Phase
0.220	28.795

exist for predicting 4P control input to minimize baseline vibrations on the basis of sampled data. The potential of these techniques, as well as others to be applied in a multiple-input, multiple-output mode, will be discussed in the next section.

Multiple Input, Multiple Output Predictive Analyses

A primary consideration in approaching higher harmonic control in a multiple-input multiple-output mode is that there exist only three independent swash-plate degrees of freedom to minimize six hub vibratory responses. One approach is to minimize just the three hub responses that largely contribute to vertical fuselage response, namely, 4P vertical forces, 4P fore-aft forces and 4P pitching moments at the hub. Alternatively, one could address the responses contributing to lateral fuselage response: 4P side forces and 4P rolling and yawing moments. However many hub forces will be minimized, once the control objective has been established the predictive algorithm must be developed.

In developing a predictive technique for this mode of harmonic control, it is desirable to again minimize sampling and data processing requirements. Thus, to simply extend the 6-point nonlinear technique to 3-inputs and 3-outputs, would require 15 input perturbations, and 48 FFT's or spectral analyses, thereby, proving too burdensome for adaptive control systems. Similarly, the three-point technique would require 6 input perturbations and 21 FFT's in a 3-input, 3-output mode. Even extending the two-point technique to such a mode would require 3 perturbations and 12 FFT's per solution update. A linear regression analysis in the frequency domain, discussed in the next section, requires three perturbations and only six FFT's and as such, hold much promise in multiple-input, multiple output applications.

Linear Regression Predictive Analysis

The analysis of a linear system with p inputs and a single output shall be considered first. By virtue of system linearity, response in the time domain can be written as a sum of p individual component responses

$$Y(t) = \sum_{k=1}^{p} Y_k(t) \qquad (12)$$

For the case of a single hub output, say normal force, and input from 3 swashplate d.o.f.s Eq. 12 becomes

$$F_z(t) = F_{z_1}(t) + F_{z_2}(t) + F_{z_3}(t) + F_{z_o}(t) \tag{13}$$

where F_{z_o} represents a baseline normal force response and $F_{zk}(t)$ represents normal force response to the k^{th} input when other inputs are zero. The individual component responses, $F_{zk}(t)$ can be represented as the convolution of the inputs $x_k(t)$ with the impulse response functions $h_k(t)$. Hence the component outputs are given as follows:

$$F_{zk}(t) = \int_{-\infty}^{\infty} h_k(\tau) x_k(t - \tau) d\tau \tag{14}$$

The Fourier transform of Eq. 14 yields

$$F_{zk}(f) = H_{k_{Fz}}(f)\, X_k(f) \tag{15}$$

where $F_{zk}(f)$ and $X_k(f)$ are the complex Fourier transforms of $F_{zk}(t)$ and $x(t)$ respectively. Thus, the Fourier transform $F_z(f)$ for the total output is,

$$F_z(f) = H_{1_{F_z}}(f)\, X_1(f) + H_{2_{F_z}}(f)\, X_2(f) + H_{3_{F_z}}(f)\, X_3(f) + F_{zo}(f) \tag{16}$$

or,

$$F_z(f) = \sum_{k=1}^{p} H_{k_{F_z}}(f) X_k(f) + F_{zo}(f) \tag{17}$$

where $F_{zo}(f)$ is the complex Fourier transform of the baseline normal force response.

Now if p independent observations of the inputs and outputs are available, then $H_{kF_z}(f)$ k = 1, 2, . . , p can be obtained by solving the linear simultaneous equation

$$F_z^{(v)}(f) = \sum_{k=1}^{p} H_{kF_z}(f) X_k^{(v)}(f) + F_{zo}(f) \qquad (18)$$

$$(v = 1, 2, . . , p)$$

where v is the observation index. As outlined in Reference 13, for the case when only a single observation is available, as would be desirable for applications to higher harmonic feathering, we can select a set of p frequencies for which the input vectors,

$$X_1(f_v) = \begin{Bmatrix} X_1(f_1) \\ X_1(f_2) \\ \cdot \\ \cdot \\ \cdot \\ X_1(f_p) \end{Bmatrix}, \quad X_2(f_v) = \begin{Bmatrix} X_2(f_1) \\ X_2(f_2) \\ \cdot \\ \cdot \\ \cdot \\ X_2(f_p) \end{Bmatrix}, \quad . \quad . \quad . \quad , \quad X_p(f_v)$$

are linearly independent. We can then obtain an approximation $\tilde{H}_{kF_z}(f)$ to $H_{kF_z}(f)$ by solving the simultaneous linear equations

$$F_z(f_v) = \sum_{k=1}^{p} \tilde{H}_{kF_z}(f) X_k(f_v) \qquad (19)$$

$$(v = 1, 2, \ldots , p)$$

Acknowledging the existence of additive noise n(t), the observed output $\overline{F}_z(t)$ is represented as

$$\overline{F}_z(t) = F_z(t) + n(t) \tag{20}$$

Taking Fourier transforms of equation 20,

$$\overline{F}_z(f) = \sum_{k=1}^{p} H_{k_{F_z}}(f)\, X_k(f) + n(f) \tag{21}$$

and thus if we solve the following equation for the unknowns $\tilde{\tilde{H}}_{k_{F_z}}(f)$ (k = 1, 2, ... p) in place of the equation for $\tilde{H}_{k_{F_z}}(f)$

$$\overline{F}_z(f_v) = \sum_{k=1}^{p} \tilde{\tilde{H}}_{k_{F_z}}(f)\, X_k(f_v) \tag{22}$$

$$(v = 1, 2, \ldots, p)$$

we get an approximation to $H_{kF_z}(f)$ contaminated with the noise $n(f_v)$.

If we assume there exists a set of frequencies $\{f_n\}$ for which $H_{kF_z}(f_\ell) = H_{k_{F_z}}$, k = 1, 2, .., p, ℓ = 1, 2, .., N, then

$$\overline{F}_z(f_\ell) = \sum_{k=1}^{p} H_{k_{F_z}} X_k(f_\ell) + n(f_\ell) \tag{23}$$

$$(\ell = 1, 2, \ldots, N)$$

implies a problem of estimating multiple regression coefficients.

Now consider the complex random noise variables $n_v (v = 1, 2, \ldots, N)$, which are mutually independently distributed with first and second moments

$$\left.\begin{aligned} E(n_v) &= 0 \\ E(\mathrm{Re}\, n_v)^2 &= E(\mathrm{Im}\, n_v)^2 = \sigma^2 \end{aligned}\right\} \tag{24}$$

and the observations are made on variables $X_{1_v}, X_{2_v}, \ldots, X_{p_v}, (v = 1, 2, \ldots, N)$ satisfying the relation

$$\overline{F}_z(f_v) = \sum_{k=1}^{p} H_{k_{F_z}} X_{kv} + n_v \tag{25}$$

$$(v = 1, 2, \ldots, N)$$

where the inputs $X_{1_v}, X_{2_v}, \ldots, X_{p_v}$ are considered to be observable non-random variables.

The probability density function L for the noise n_v is given as follows:

$$L = \left(\frac{1}{2\pi\sigma^2}\right)^N \exp\left(-\frac{1}{2\sigma^2}\sum_{v=1}^{N} n_v{}^2\right) \tag{26}$$

Substituting for n_v from equation 25, we obtain

$$L = \left(\frac{1}{2\pi\sigma^2}\right)^N \exp\left(-\frac{1}{2\sigma^2}\sum_{v=1}^{N}\left|\overline{F}_z(f_v) - \sum_{k=1}^{p} H_{k_{F_z}} X_k(f_v)\right|^2\right) \tag{27}$$

The maximum probability estimate, according to Reference 13, $(\tilde{H}_{1F_z}, \tilde{H}_{2F_z}, \ldots, \tilde{H}_{pF_z})$ of $(H_{1F_z}, H_{2F_z}, \ldots, H_{pF_z})$ is obtained by finding the values of H_{kF_z} which minimize the sum of squares in the second parenthesis of the right hand side of equation 27. These values are given as follows:

$$\begin{bmatrix} \tilde{H}_{1F_z} \\ \hat{H}_{2F_z} \\ \vdots \\ \tilde{H}_{pF_z} \end{bmatrix} = D^{-1} \begin{bmatrix} (\overline{F}_z, X_1) \\ (\overline{F}_z, X_2) \\ \vdots \\ (\overline{F}_z, X_p) \end{bmatrix} \tag{28}$$

where

$$D = \begin{bmatrix} (X_1, X_1)\,(X_2, X_1) \ldots (X_p, X_1) \\ (X_1, X_2)\,(X_2, X_2) \ldots (X_p, X_2) \\ \vdots \\ (X_1, X_p)\,(X_2, X_p) \ldots (X_p, X_p) \end{bmatrix} \tag{29}$$

and the inner products are defined by

$$(X_j, X_\ell) = \sum_{v=1}^{N} X_{jv} X_{\ell v}^{*} \tag{30}$$

$$(j, \ell = 1, 2, \ldots, p)$$

$(\ )^*$ denotes complex conjugate

and it is assumed that $N \geq p$ and D^{-1} exists, and for our case, $(p = 3)$,

X_{1v} = FFT of swashplate collective inputs at frequency f_v

X_{2v} = FFT of swashplate lateral cyclic inputs at frequency f_v

X_{3v} = FFT of swashplate longitudinal cyclic inputs at frequency f_v

If the above analysis is performed twice again, one each for hub pitching moment and axial force, we obtain

$$\tilde{H}_{M_y} = D^{-1} \begin{bmatrix} (\overline{M}_y, X_1) \\ (\overline{M}_y, X_2) \\ \vdots \\ (\overline{M}_y, X_p) \end{bmatrix} \tag{31}$$

$$\tilde{H}_{F_x} = D^{-1} \begin{bmatrix} (\overline{F}_x, X_1) \\ (\overline{F}_x, X_2) \\ \vdots \\ (\overline{F}_x, X_p) \end{bmatrix} \tag{32}$$

By superposing the 3 matrix systems above, we may write

$$\left\{ \tilde{H}_{F_z}, \tilde{H}_{M_y}, \tilde{H}_{F_x} \right\} = D^{-1} \begin{bmatrix} (\overline{F}_z, X_1) & (\overline{M}_y, X_1) & (\overline{F}_x, X_1) \\ (\overline{F}_z, X_2) & (\overline{M}_y, X_2) & (\overline{F}_x, X_2) \\ (\overline{F}_z, X_3) & (\overline{M}_y, X_3) & (\overline{F}_x, X_3) \end{bmatrix} \tag{33}$$

$(3 \times 3) \qquad (3 \times 3) \qquad (3 \times 3)$

Thus, equation 16 can be extended to include three hub outputs as follows:

$$\begin{Bmatrix} \overline{F}_z(f) - F_{zo}(f) \\ \overline{M}_y(f) - M_{yo}(f) \\ \overline{F}_x(f) - F_{xo}(f) \end{Bmatrix} = \begin{Bmatrix} H_{F_z}, & H_{M_y}, & H_{F_x} \end{Bmatrix} \begin{Bmatrix} X_1(f) \\ X_2(f) \\ X_3(f) \end{Bmatrix} \tag{34}$$

The higher harmonic solution input is obtained by setting $\overline{F}_z$, $\overline{M}_y$ and $\overline{F}_x$ to zero, inverting the complex transfer function matrix and multiplying:

$$\begin{Bmatrix} X_1(f) \\ X_2(f) \\ X_3(f) \end{Bmatrix}^* = \begin{Bmatrix} H_{F_z}, & H_{M_y}, & H_{F_x} \end{Bmatrix}^{-1} \begin{Bmatrix} -F_{zo}(f) \\ -M_{yo}(f) \\ -F_{xo}(f) \end{Bmatrix} \tag{35}$$

where * now denotes an optimal solution.

It is seen that the transfer function generated in this estimation technique can be used to relate 3/rev, 4/rev, and 5/rev harmonic blade pitching to similar harmonics of blade flapwise and edgewise root shears. Writing third, fourth, and fifth harmonic blade pitching in terms of fourth harmonic swashplate pitching, rolling and collective motion in addition to solving for similar harmonics of blade root shears in terms of fourth harmonic hub forces and moments permits the direct application of equation 33. Once an objective function is written in terms of swashplate displacements and hub forces and moments, optimal swashplate inputs required to null certain hub vibratory forces can be derived, as in equation 35. Reference 13 presents details for the construction of a confidence region for the estimate of the frequency response function at a given frequency. In addition, special smoothing and filtering techniques may be necessary to improve the statistical nature of the sampled data. Reference 12 lists several frequency domain techniques for smoothing raw spectra.

The anticipated control sequence for applying such an algorithm involves measuring 3 hub baseline vibration levels to initiate the solution procedure. Once the ambient or baseline levels have been determined, a single simultaneous swashplate perturbation in pitch, roll and collective at 4P yields

information necessary to generate required inputs for nulling the baseline condition. The dependency of such ambient vibration levels upon flight condition requires that the solution feathering inputs be updated in response to changes in rotor trim. It would be undesirable, however, to render the actuator system idle each time baseline levels are to be obtained for a solution refresh. An alternate control scheme might consist of working with finite differences to minimize, not the baseline response, but the change in hub response due to changes in rotor trim. That is, once optimal swashplate inputs have been derived and implemented, there exists a minimized but finite residual hub response. As these vibratory loads increase in response to changes in rotor trim, the control objective becomes one of minimizing the "delta" such as to drive hub loads back to the original minimized level. This technique would, therefore, preclude idling the actuators each time rotor trim is changed.

Note here that the envisioned adaptive control network design shall not address alleviation of helicopter gust response. Not only are rotors highly effective gust attenuators in their present form, but the low frequency spectral content of gust response quantities is not amenable to attenuation with fourth harmonic feathering.

The solution algorithms presented here will be evaluated in upcoming wind tunnel investigations of multiple-input, multiple-output higher harmonic control of NASA/Langley Research Center.

Conclusions

Data obtained from a recent wind tunnel investigation of single-input, single-output higher harmonic control has led to the following conclusions.

- By varying phase and amplitude of 4P collective, lateral cyclic or longitudinal cyclic feathering, the 4P spectral component of any of six rotor-transmitted hub oscillatory responses can be minimized for a given trim condition.

- 4P collective inputs needed to minimize 4P hub normal forces induce higher peak-to-peak torsional moments and, hence, pitch link loads on an articulated rotor.

- Flapwise and chordwise bending moments were fairly insensitive to "optimal" 4P collective inputs, on the rotor tested.

An investigation of several techniques for predicting 4P swashplate inputs needed to minimize 4P hub vibratory responses using wind tunnel test data has generated the following conclusions:

- There exists an almost linear relationship between 4P hub responses and 4P feathering inputs.

- Optimal single inputs can be generated from vibratory response data. Such inputs can be calculated from a completely general 6-point nonlinear algorithm. However, by taking advantage of several key assumptions, a computationally more efficient technique can be derived requiring only 2 sample response data points.

- Techniques exist for treating the multiple-input, multiple-output mode of higher harmonic control. The effectiveness of these algorithms will be assessed in an upcoming wind tunnel program.